

## Научный семинар






**materials**



*Article*

# The Analysis of Superelasticity and Microstructural Evolution in NiTi Single Crystals by Molecular Dynamics

Hung-Yuan Lu <sup>1</sup> , Chih-Hsuan Chen <sup>2</sup>  and Nien-Ti Tsou <sup>1,\*</sup> 



# Постановка задачи: начальная структура

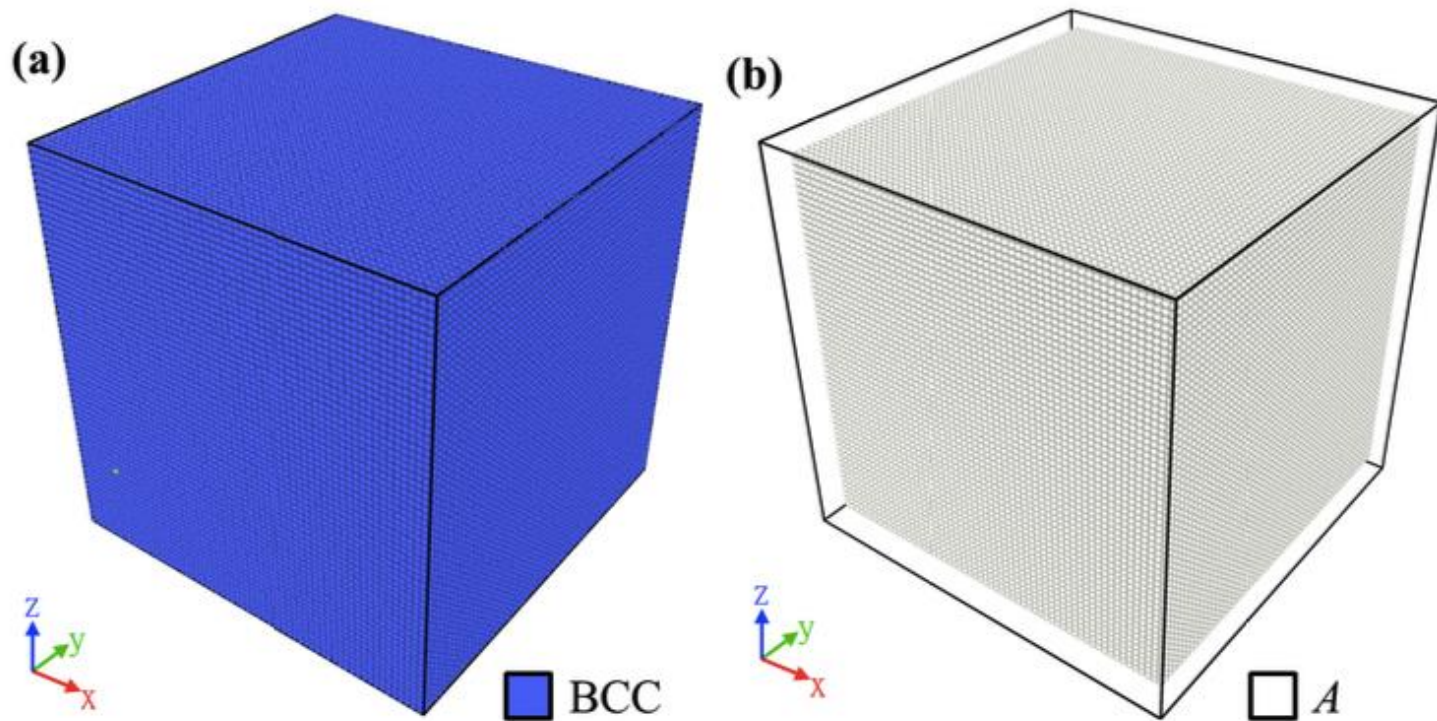


**Figure 2.** A typical example of the results at the initial step of the compression tests, analyzed and visualized with (a) polyhedral template matching (PTM) and (b) the martensite variant identification.



# Примеры визуализации структуры

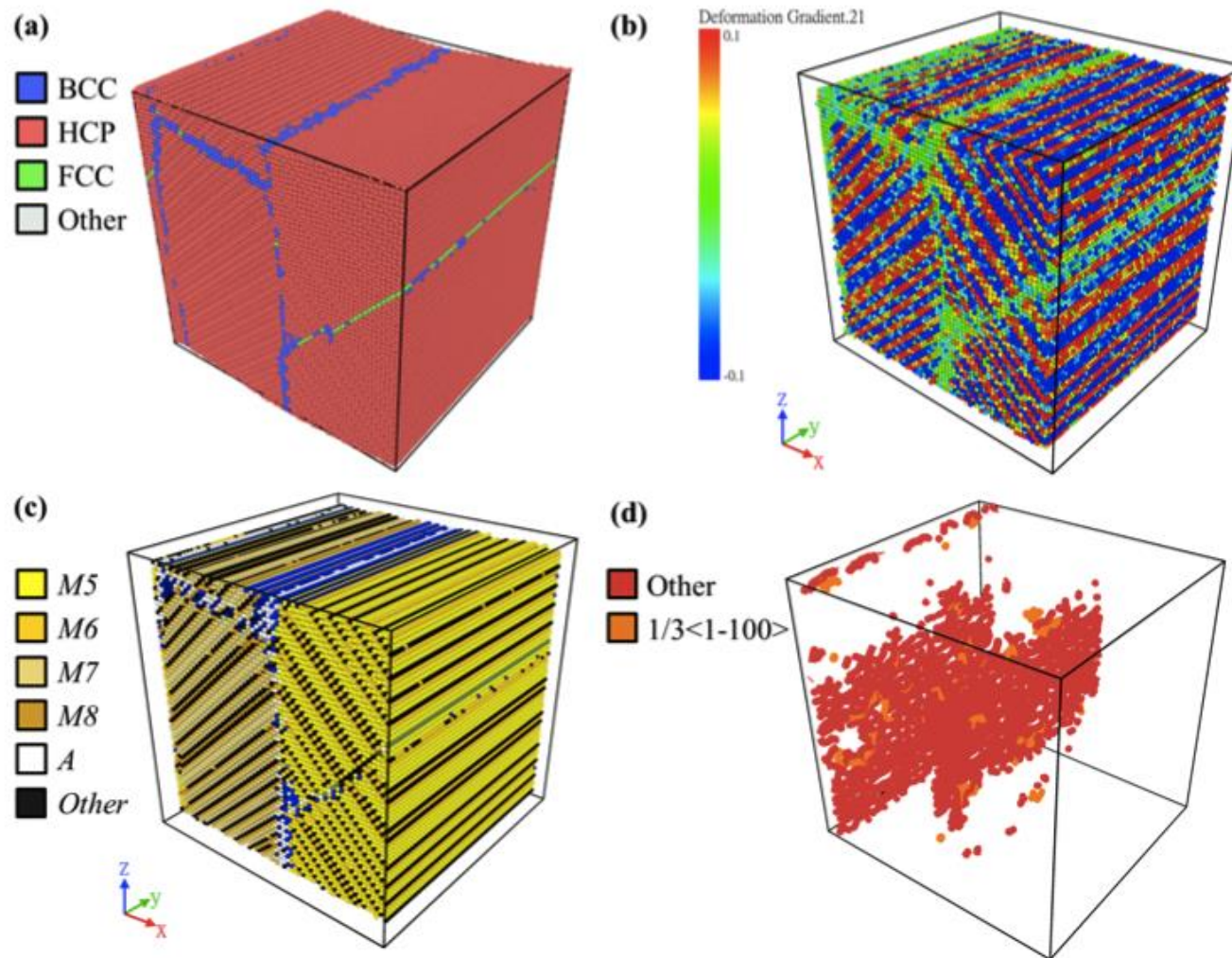


**Figure 3.** A typical example of the results during the compression tests, analyzed and visualized with (a) PTM, (b) the deformation gradient, (c) the martensite variant identification, and (d) DXA (dislocation analysis) methods.



# Постановка задачи: потенциалы

The simulations were performed by a well-known MD package, LAMMPS (Large-scale Atomic/Molecular Massively Parallel Simulator) [18]. The interatomic potential of NiTi was described by the 2NN MEAM potential energy [19].

The periodic boundary condition (PBC) was applied in all three directions,  $x$ ,  $y$ , and  $z$ . The atom arrangement was then relaxed at 0 K by the conjugate gradient method in order to minimize the total energy and to eliminate the internal stress. Next, the model underwent the thermal equilibrium at 325 K for 40 ps (20,000 time steps); where the velocities were assigned to atoms by the Gaussian distribution based on the given temperature.

Note that the given temperature 325 K, which is between the austenite finish temperature ( $A_f$ ) and the martensite start temperature ( $M_s$ ), was chosen here to obtain a more stable stress-induced martensitic transformation between austenite and martensite phases in the simulation. For each case, the time step was 2 fs, and the constant temperature was controlled by the isothermal-isobaric (NPT) canonical ensemble along with a pressure of 1.013 bar. After the thermal equilibrium stage, the deformation of the material was controlled by the strain rate of the simulation box.





# Кривые напряжение-деформация

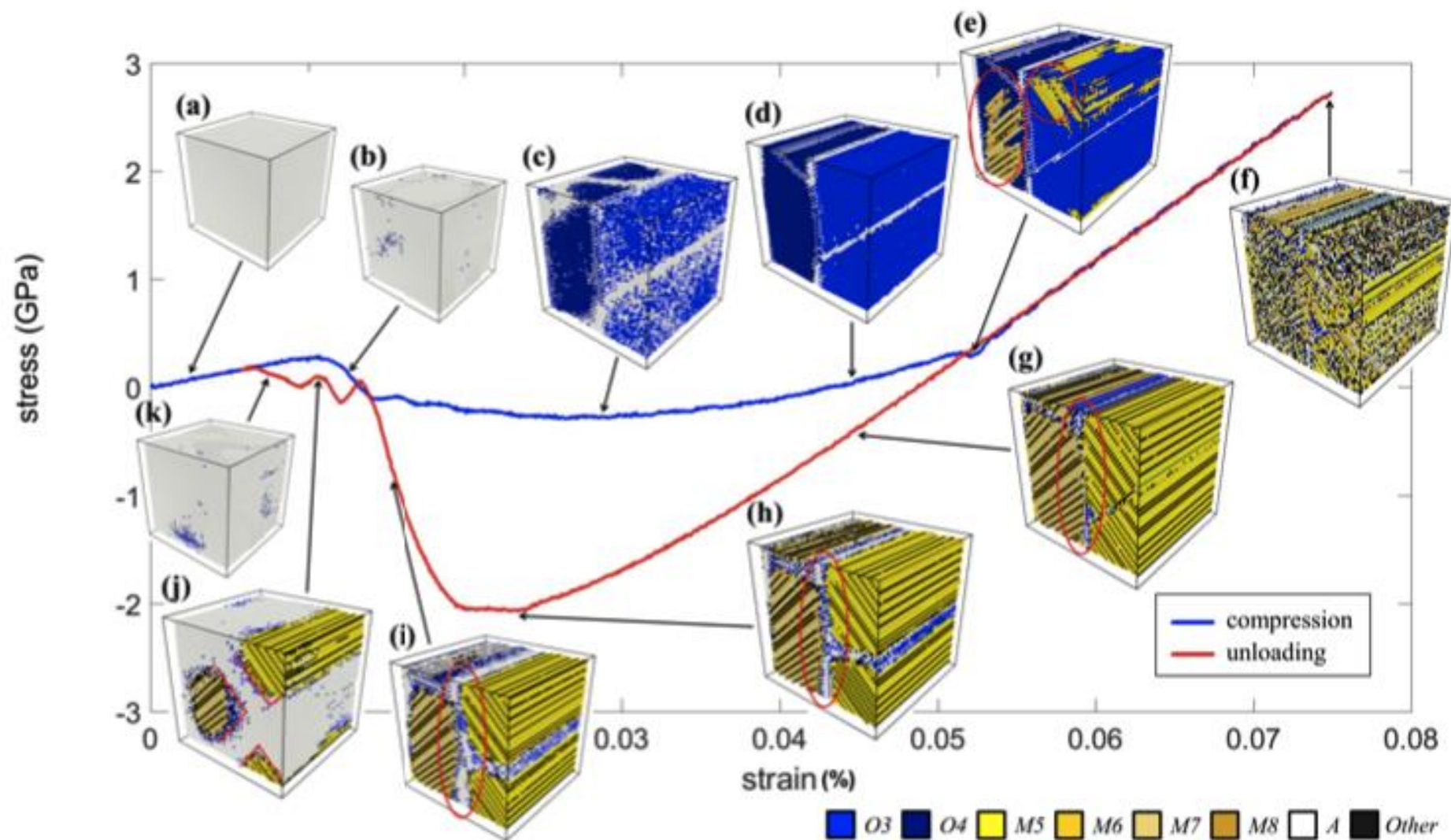
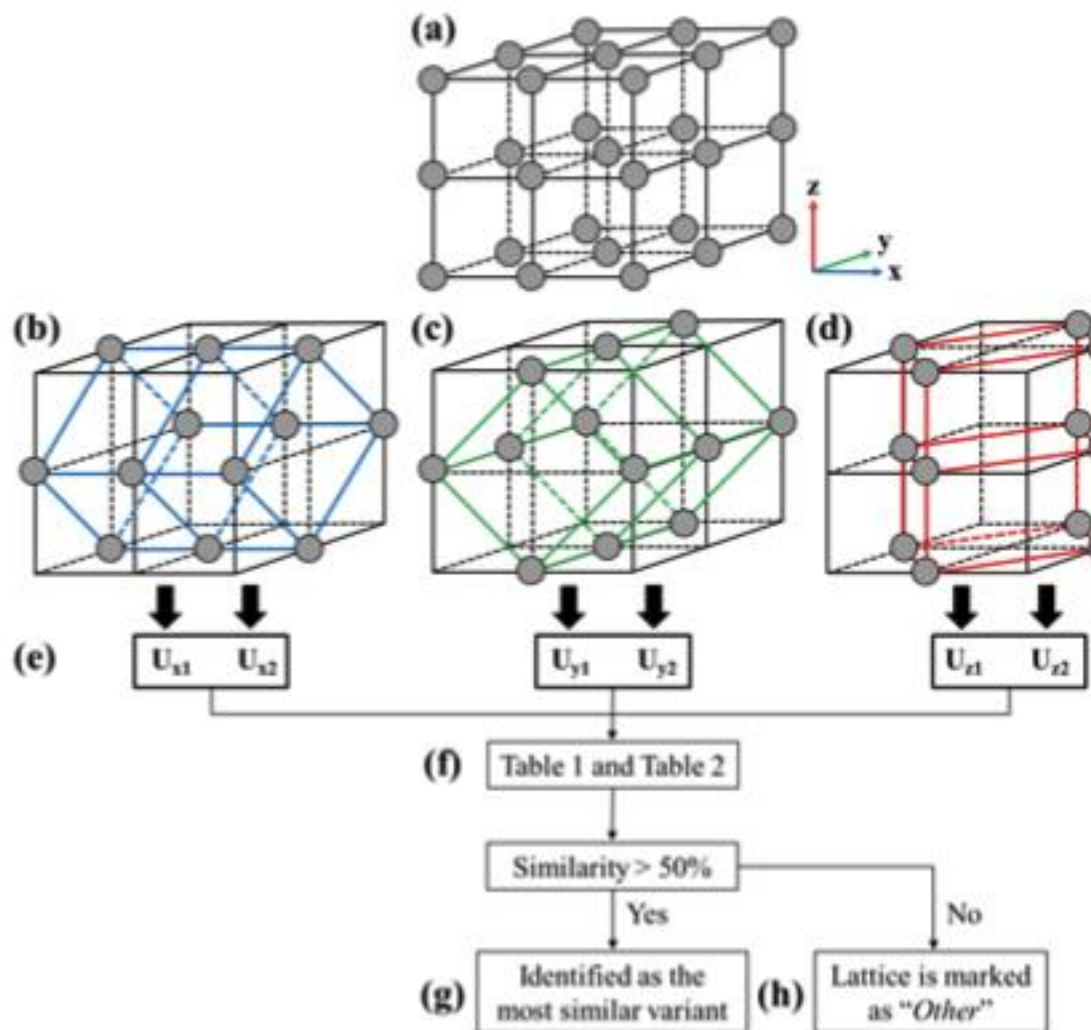


**Figure 4.** The stress–strain curve of the NiTi shape memory alloy (SMA) subjected to the compression process. The corresponding microstructures at stages (a–k) are shown.

# Фазы



Condition ID	Conditions
A	$u_{11} - 1 \geq \phi$
B	$u_{22} - 1 \geq \phi$
C	$u_{33} - 1 \geq \phi$
D	$u_{11} - 1 < \phi$
E	$u_{22} - 1 < \phi$
F	$u_{33} - 1 < \phi$
G	$u_{12} \geq \phi$
H	$u_{13} \geq \phi$
I	$u_{23} \geq \phi$
J	$u_{12} \leq -\phi$
K	$u_{13} \leq -\phi$

Variant No.	Conditions to be Satisfied
M1	B, C, D, I, J, K, M
M2	B, C, D, G, H, I, M
M3	B, C, D, G, K, L, M
M4	B, C, D, H, J, L, M
M5	A, C, E, H, J, L, N
M6	A, C, E, G, H, I, N
M7	A, C, E, G, K, L, N
M8	A, C, E, I, J, K, N
M9	A, B, F, G, K, L, O
M10	A, B, F, G, H, I, O
M11	A, B, F, I, J, K, O
M12	A, B, F, H, J, L, O
O1	B, C, D, I
O2	B, C, D, L
O3	A, C, E, H
O4	A, C, E, K
O5	A, B, F, G
O6	A, B, F, J
A	M, N, O

$\leq \phi$   
 $\leq \phi$   
 $\leq \phi$



# Изменение энергии

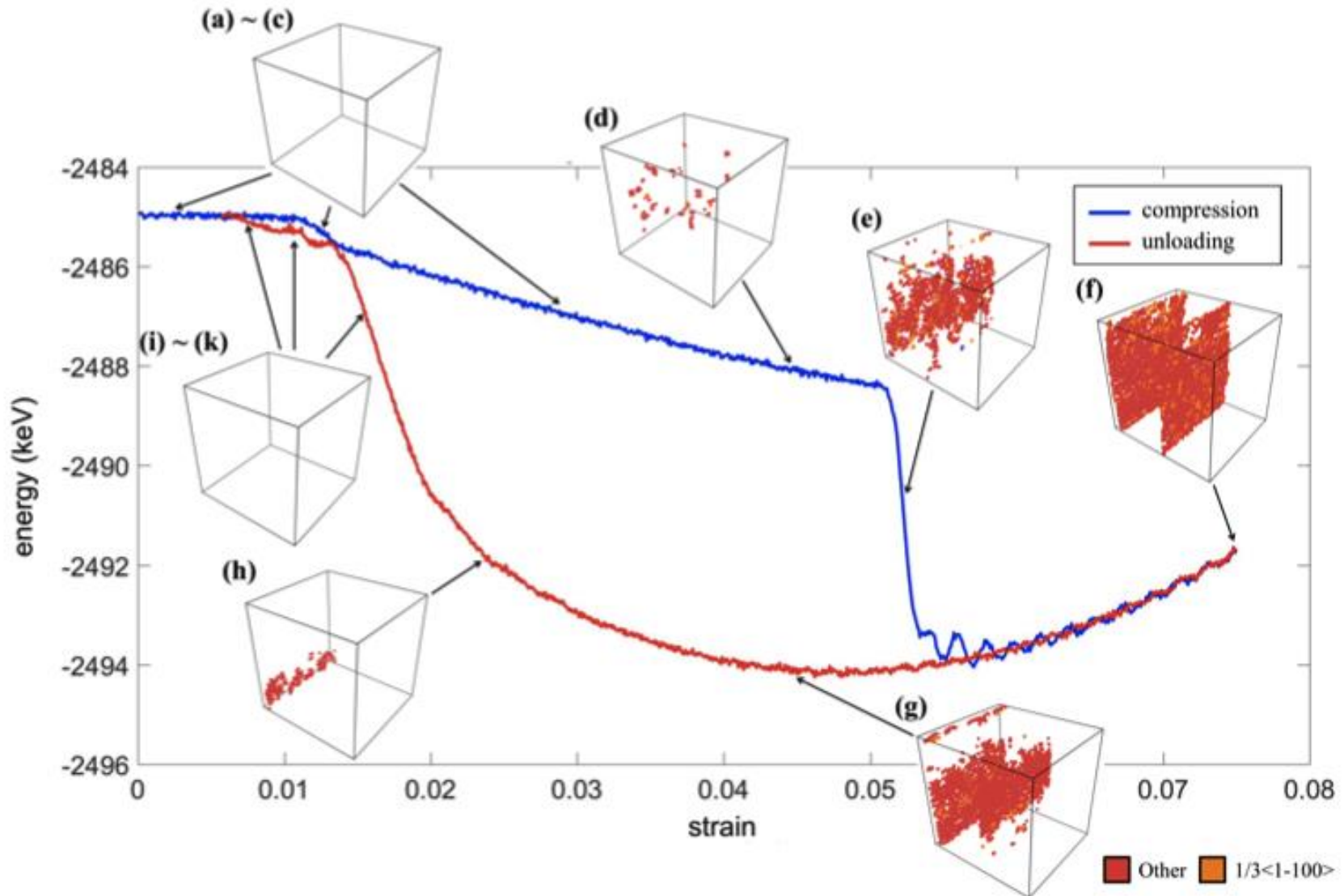
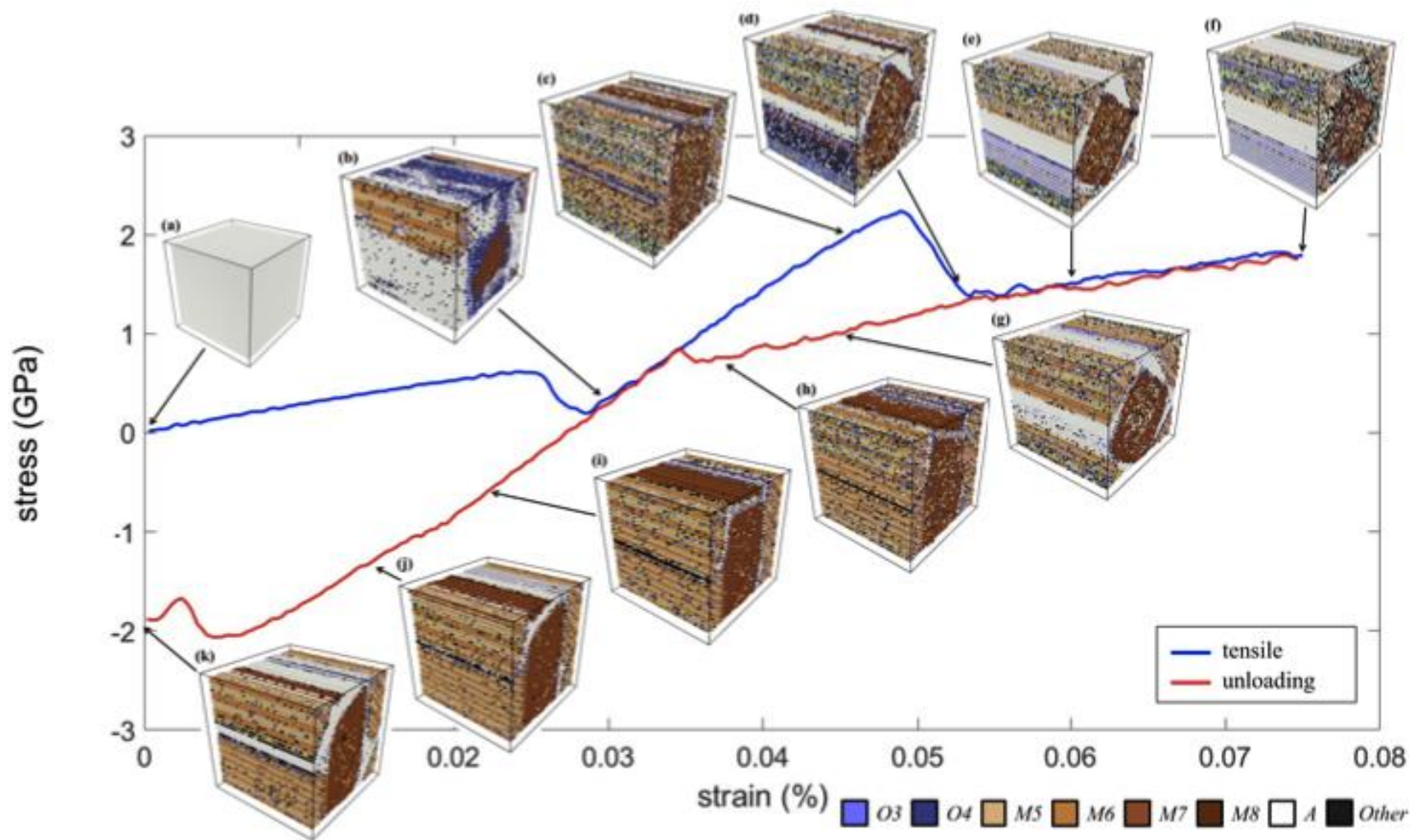


Figure 5. The energy profile and the evolution of dislocation at stages (a–k) during the compressive loading.



# Растяжение



**Figure 6.** The stress–strain curve of the NiTi SMA subjected to tensile loading. The corresponding microstructures at Stages (a–k) are shown.





# Структурные перестройки

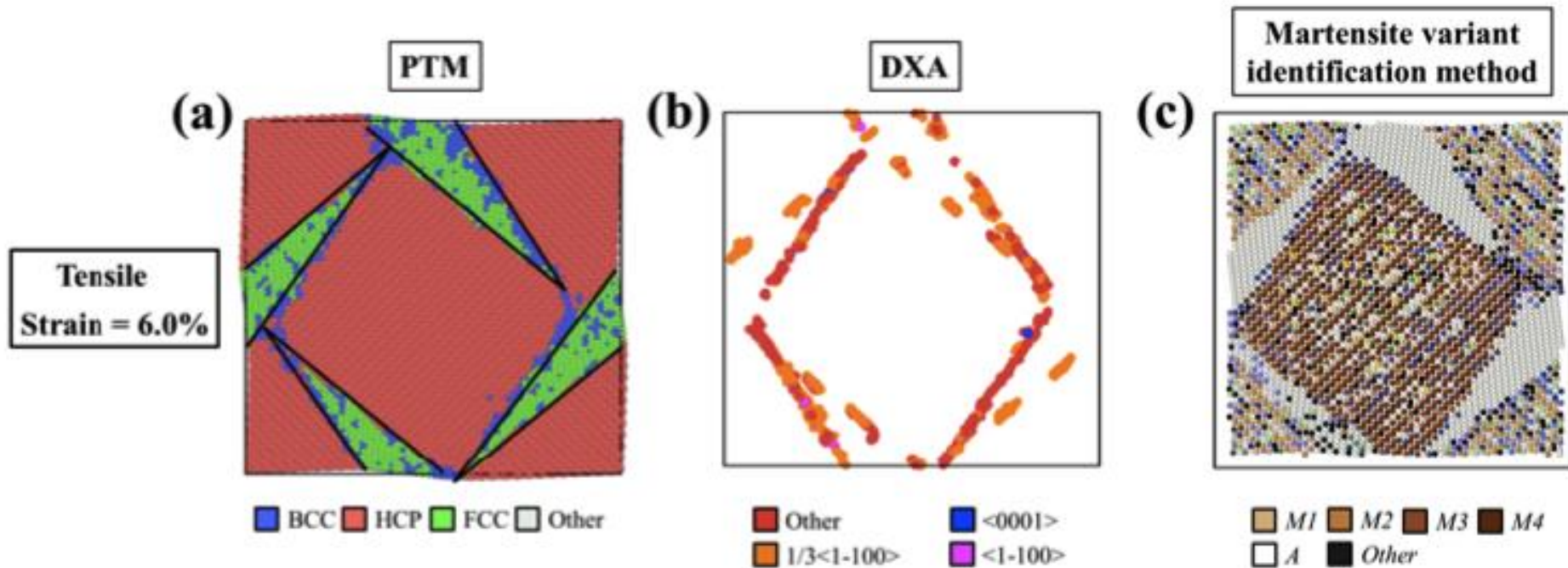


**Figure 7.** The self-accommodating microstructure induced at the tensile strain of 6%, visualized by (a) PTM, (b) DXA (dislocation analysis), and (c) the martensite variant identification methods.



# Распределение энергии при растяжении

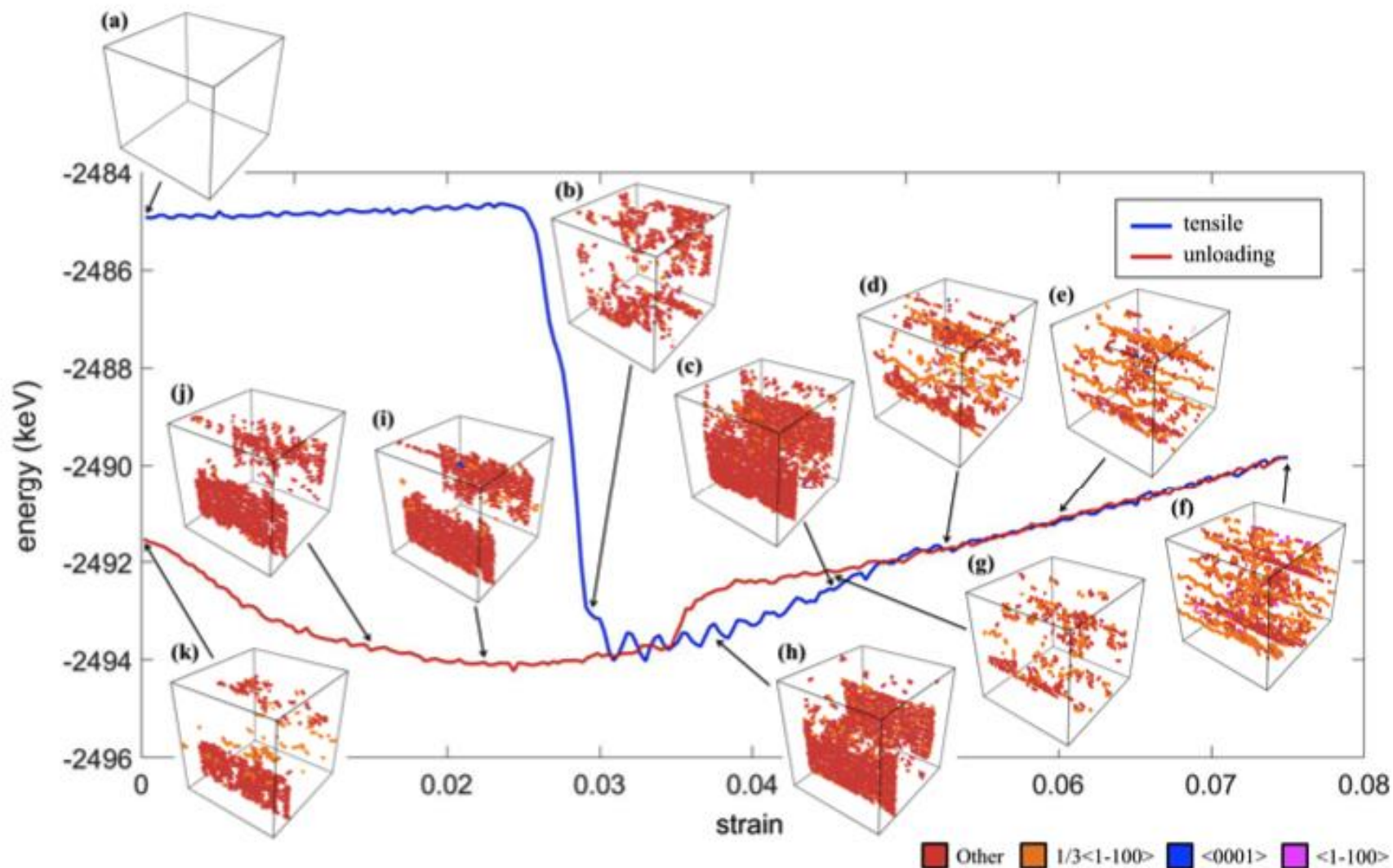


**Figure 8.** The energy profile and the evolution of dislocation at Stages (a–k) during the tensile loading along the  $y$  axis.



# Сдвиговая деформация

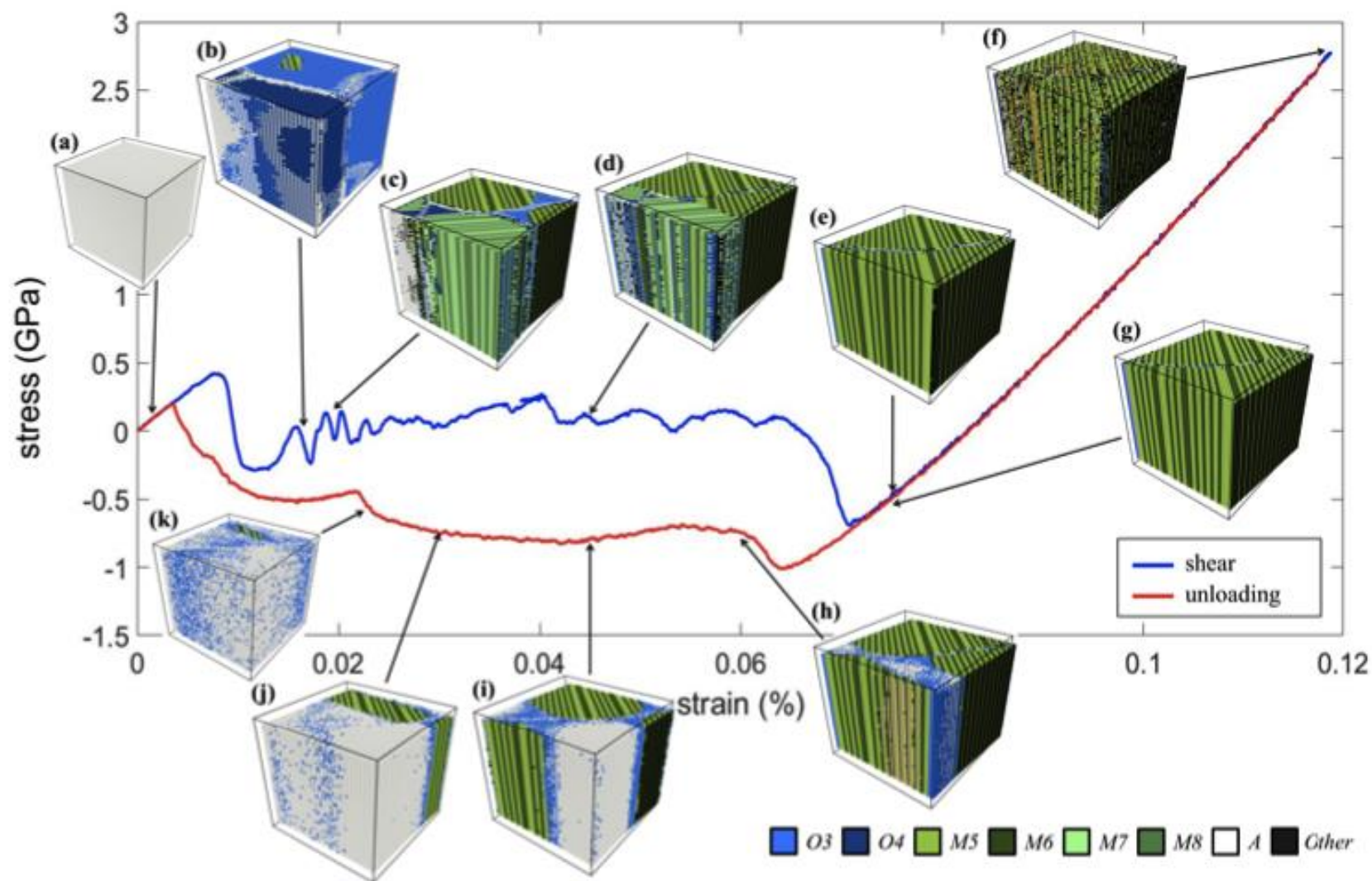


**Figure 9.** The stress-strain curve of the NiTi SMA subjected to the  $xy$  shearing load. The corresponding microstructures at Stages (a–k) are shown.





# Распределение энергии при сдвиге

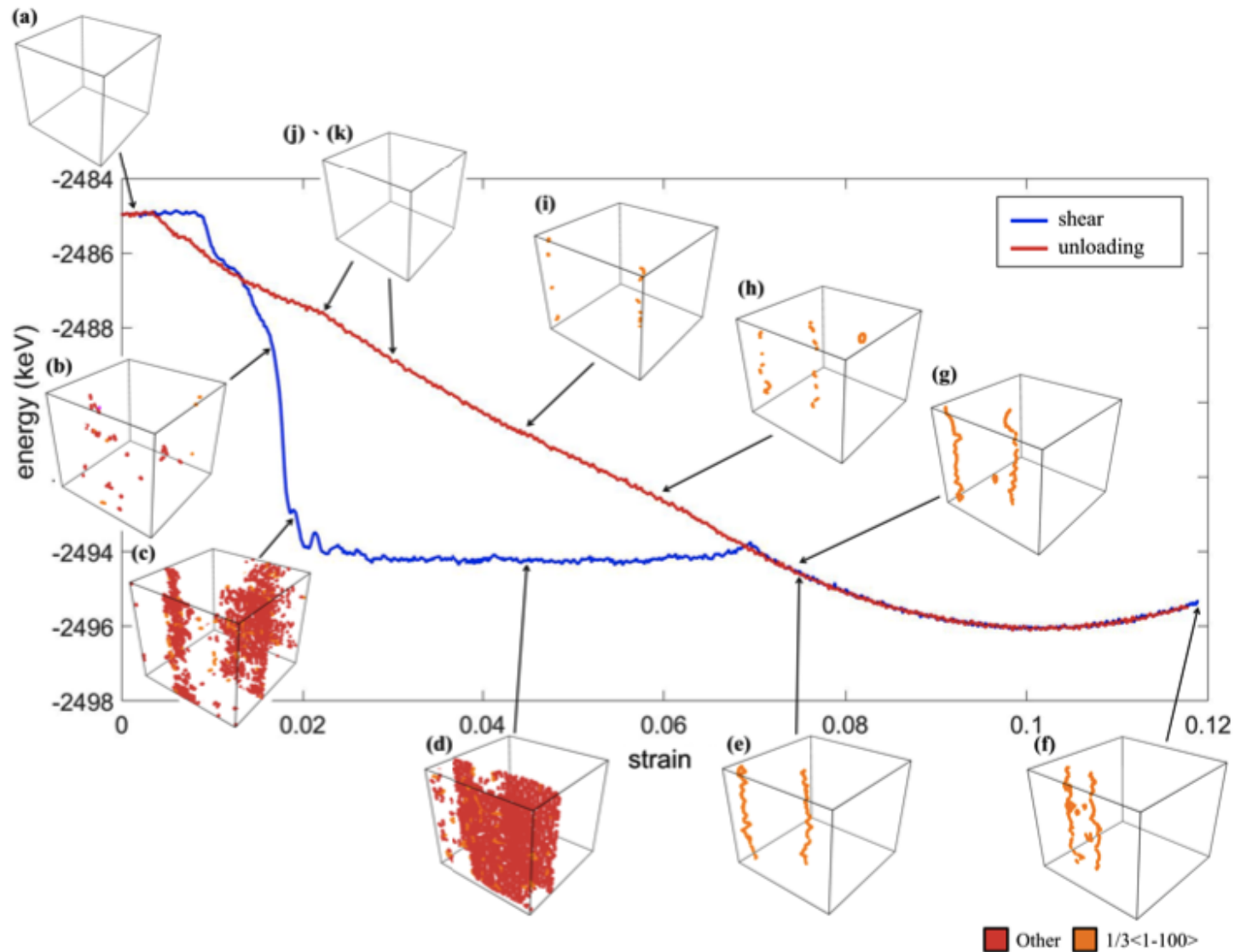


Figure 10. The energy profile and the evolution of dislocation at Stages (a–k) during the  $xy$  shearing.



# ВЫВОДЫ

The uniaxial compression, tensile, and shearing tests for NiTi alloys were studied by MD simulations in the current work. The relationship between the interface compatibility in NiTi and the dislocation accumulation was also discussed. The tendency of the onset of martensitic transformation for the shearing, compression, and tensile tests (from low to high) was also accurately predicted.

Our simulations also showed that the superelasticity of the NiTi single crystal was significant for the shear and compression loading and was not obvious for the tensile case. By using three post-processing methods, PTM, DXA, and the martensite variant identification method, the microstructures with wedge-shaped regions of the stressed austenite phase were revealed.

The special microstructure accumulated dislocations on the twin boundaries and is expected to be the cause of the reduction of the superelasticity of NiTi under the tensile loads.

The relationship between energy profile and dislocation distribution was also discussed.

